Molecular Cell, Volume *76*

Supplemental Information

RNA Interactions Are Essential for CTCF-Mediated Genome Organization

Ricardo Saldaña-Meyer, Javier Rodriguez-Hernaez, Thelma Escobar, Mayilaadumveettil Nishana, Karina Jácome-López, Elphege P. Nora, Benoit G. Bruneau, Aristotelis Tsirigos, Mayra Furlan-Magaril, Jane Skok, and Danny Reinberg

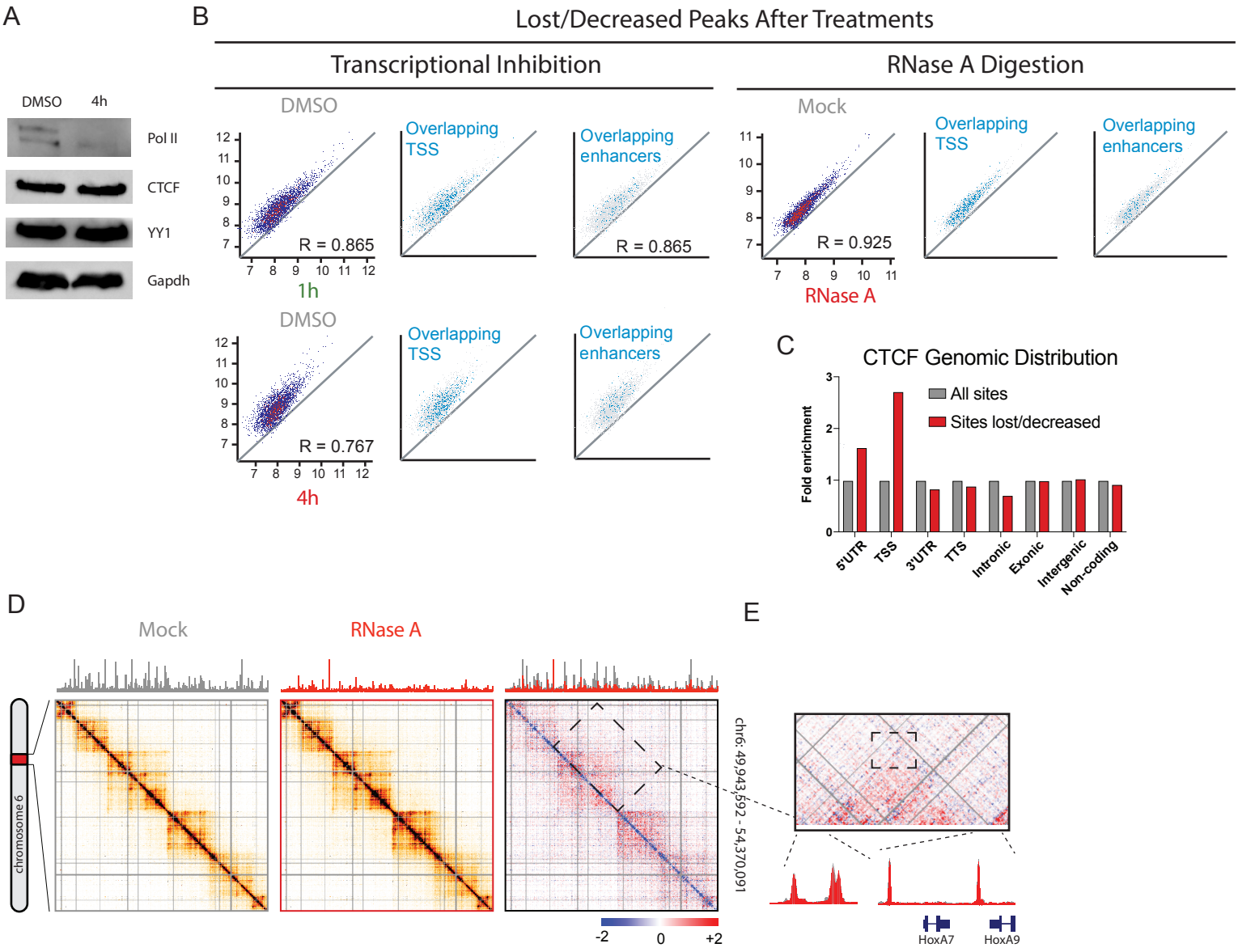

Figure S1 related to Figure 1. Transcriptional inhibition disrupts CTCF binding predominantly in TSS. mESCs were incubated with a combination of transcriptional inhibitors (Triptolide and DRB; TI) for 4 hr or with RNase A digestion. (A) Immunoblot for proteins shown in control (DMSO) versus TI (4hr). (B) A subset of peaks dramatically reduces CTCF enrichment in TI and RNase A digestion. Overlapping peaks for TSS and enhancers are shown in blue for each condition. (D) Bar graph comparing the fold-enrichment of the genomic distribution of CTCF binding sites in the control against those binding sites significantly decreased with TI and RNase A. (D) 5C heatmap depicting the interaction frequency between restriction fragments across a 4-Mb region surrounding the HoxA cluster (data were binned in 15-kb windows; step size 5 kb; the median is shown). Darker colors represent increasing interaction frequency. (E) Zoom into a chromatin domain delimited by CTCF sites (top). Overlapping ChIP-Seq tracks for Mock (grey) and RNase A digestion (red) illustrate no change in CTCF binding for the loop enclosed in a rectangle (bottom).

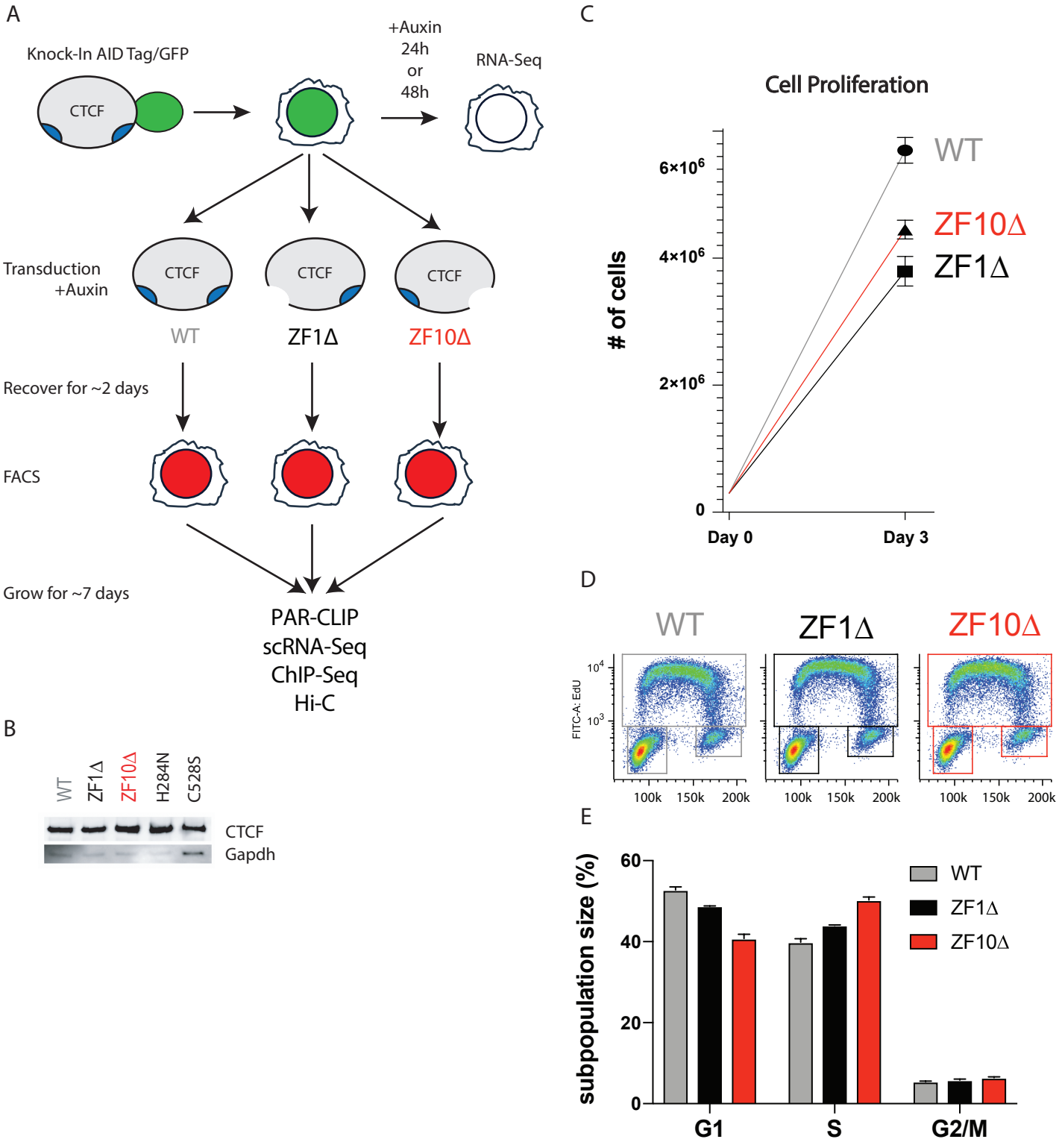

Figure S2 related to Figure 2. Mutations in ZF1 and ZF10 independently abolish CTCF binding to RNA.

(A) Schematic representation of the cell lines and approaches used. (B) Immunoblot showing CTCF levels in the rescue cell lines as indicated. (C) Growth curve showing the difference in proliferation after rescue with the different mutants as indicated, compared to rescue with WT (n=2). (D) Flow analysis showing EdU and Propidium Iodide staining (E) Percentages of cell-cycle subpopulations from (D) highlighting cells in G1-, S-, and G2/M stages.

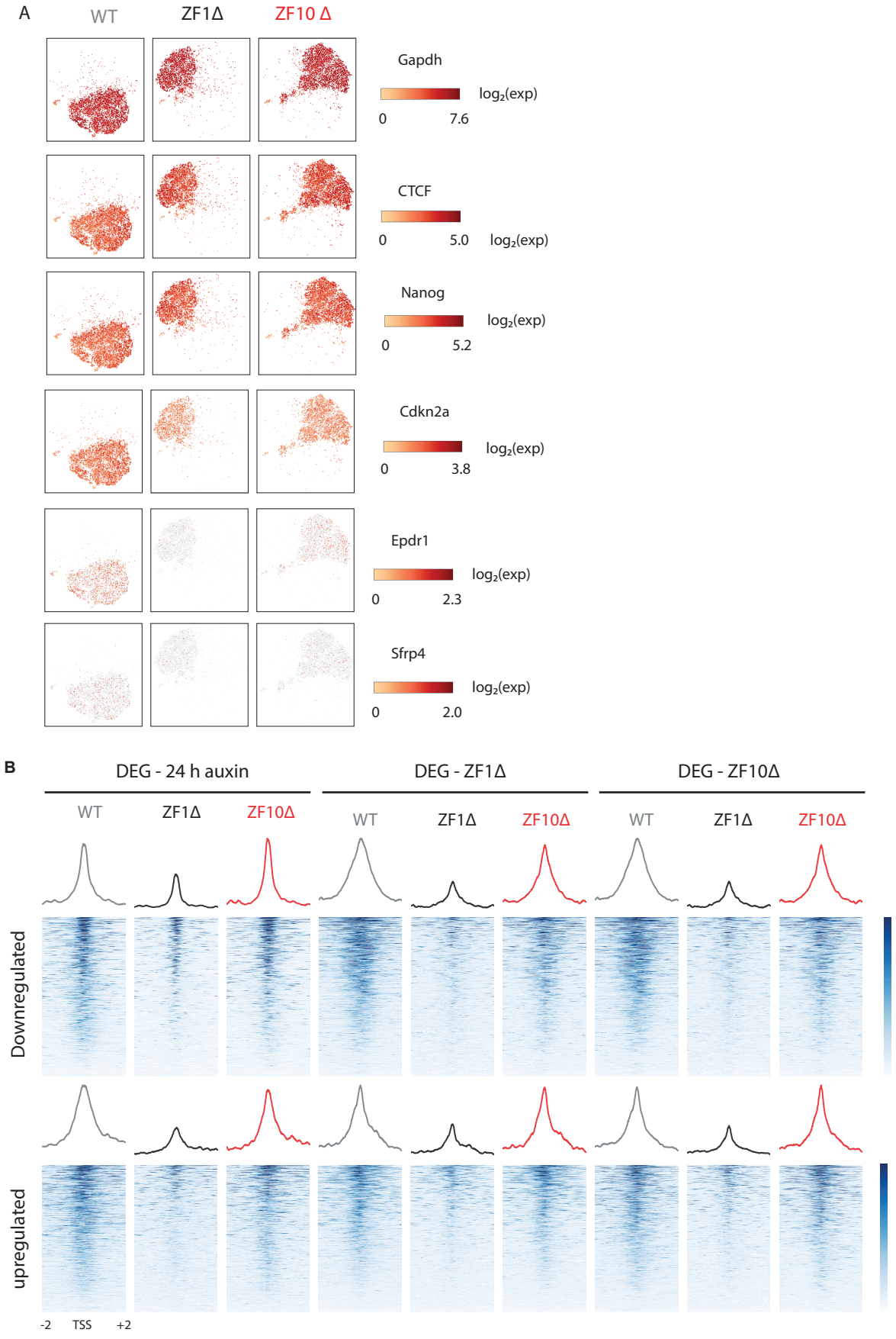

Figure S3 related to Figure 3. Gene expression defects correlate with CTCF chromatin binding.

(A) Expression of the genes shown as measured by single-cell RNA-Seq of rescue cell lines. Each dot represents a single-cell and dots are shaded based on their normalized expression value. (B) CTCF ChIP-seq for each rescue cell line indicated. Heatmaps were generated by centering and rank-ordering on DEG for each condition shown. Corresponding average density profiles are plotted at the top of the heatmaps.

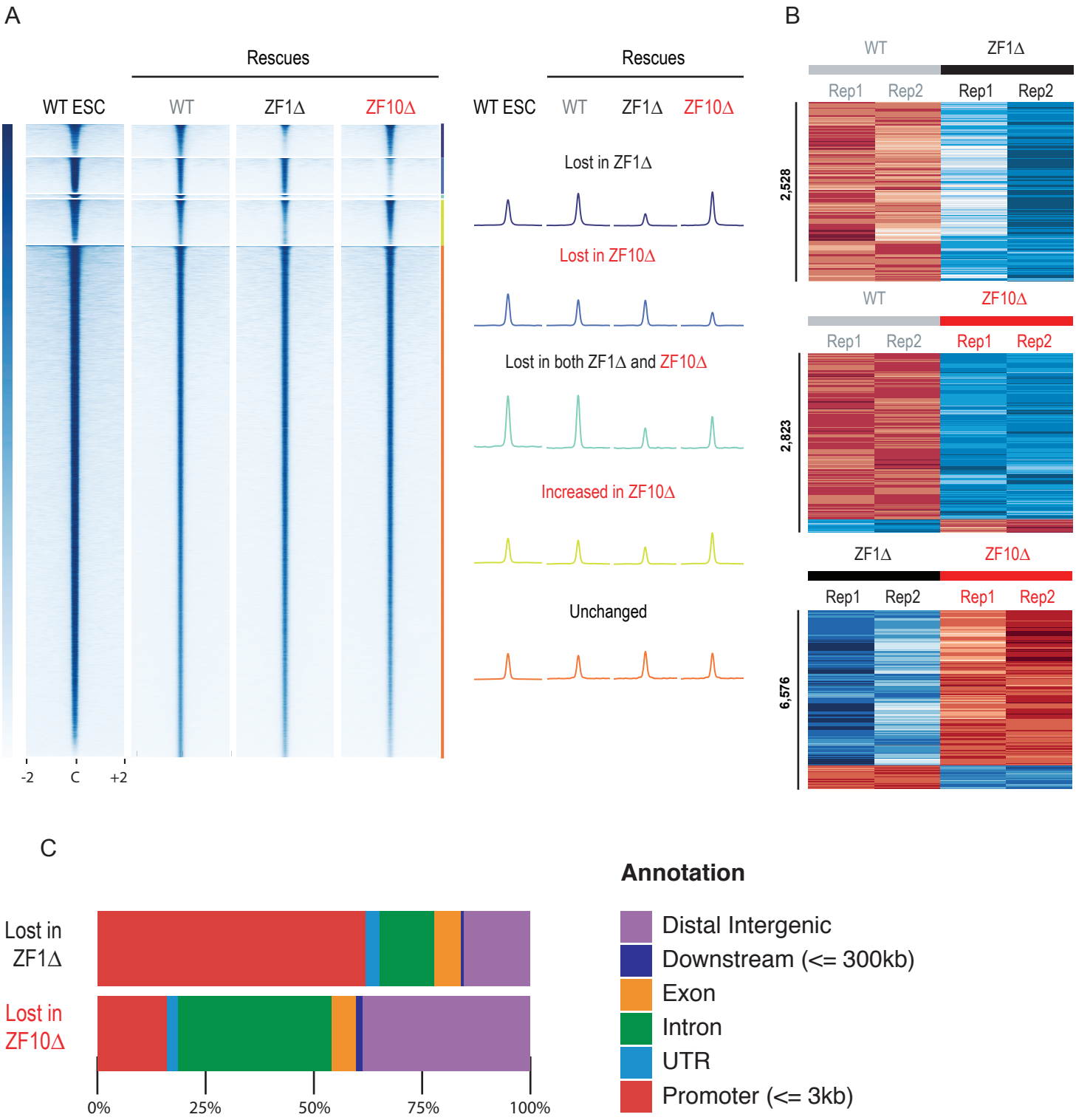

Figure S4 related to Figure 4.
(A) CTCF ChIP-seq for WT (grey), ZF1Δ (black) and ZF10Δ (red) rescue cell lines and a WT ESC control. Heatmaps were generated by centering and rank-ordering on CTCF binding sites by sub-group. Average density profiles are shown on the right for each sub-group. (B) Heatmap showing differential CTCF peaks identified using DiffBind analysis of ChIP-seq duplicates in WT vs ZF1Δ (top), WT vs ZF10Δ (middle), and ZF1Δ vs ZF10Δ (bottom). Increases and decreases in CTCF binding are shown in red and blue, respectively. (C) Comparison of genomic locations for differential CTCF peaks for ZF1Δ and ZF10Δ.

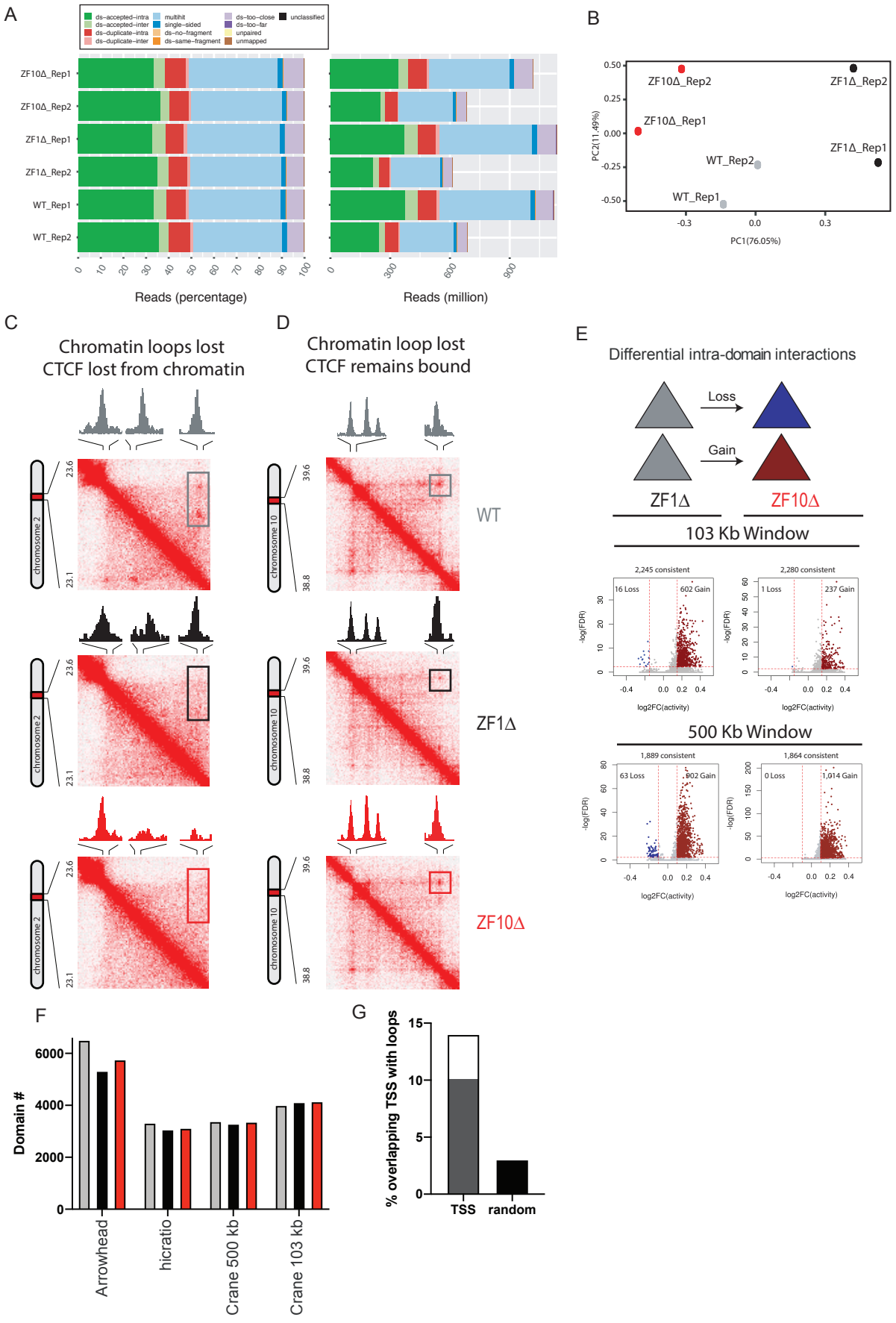

Figure S5 related to Figure 5. RBR mutants disrupt 3D organization

(A) Mapping and sequencing summary for all replicates and conditions. (B) PCA for all replicates and conditions. (C) Representative contact matrix (at 5 kb resolution) show that two chromatin loops in the WT rescue (left) disappear in ZF1Δ (middle) and ZF10Δ (right), while CTCF binding is lost at two of the anchors in ZF10Δ only. (D) Same as (C) but in this example the chromatin loop in the WT rescue (left) loses strength in ZF1Δ (middle) and ZF10Δ (right) while CTCF remains bound under all conditions. (E) Intra-domain interaction changes in WT vs ZF1Δ and WT vs ZF10Δ for common domains called by Crnae at 103 or 500 kb windows. CTCF mutant rescues are associated with gain (red) and loss (blue) of intra-domain interactions. (F) Chromatin domains called by the different algorithms indicated. (G) Percentage of overlap of TSS with all chromatin loops annotated for the WT rescue (TSS located in the anchors of a chromatin-interacting domain are highlighted in grey) compared to a random control.

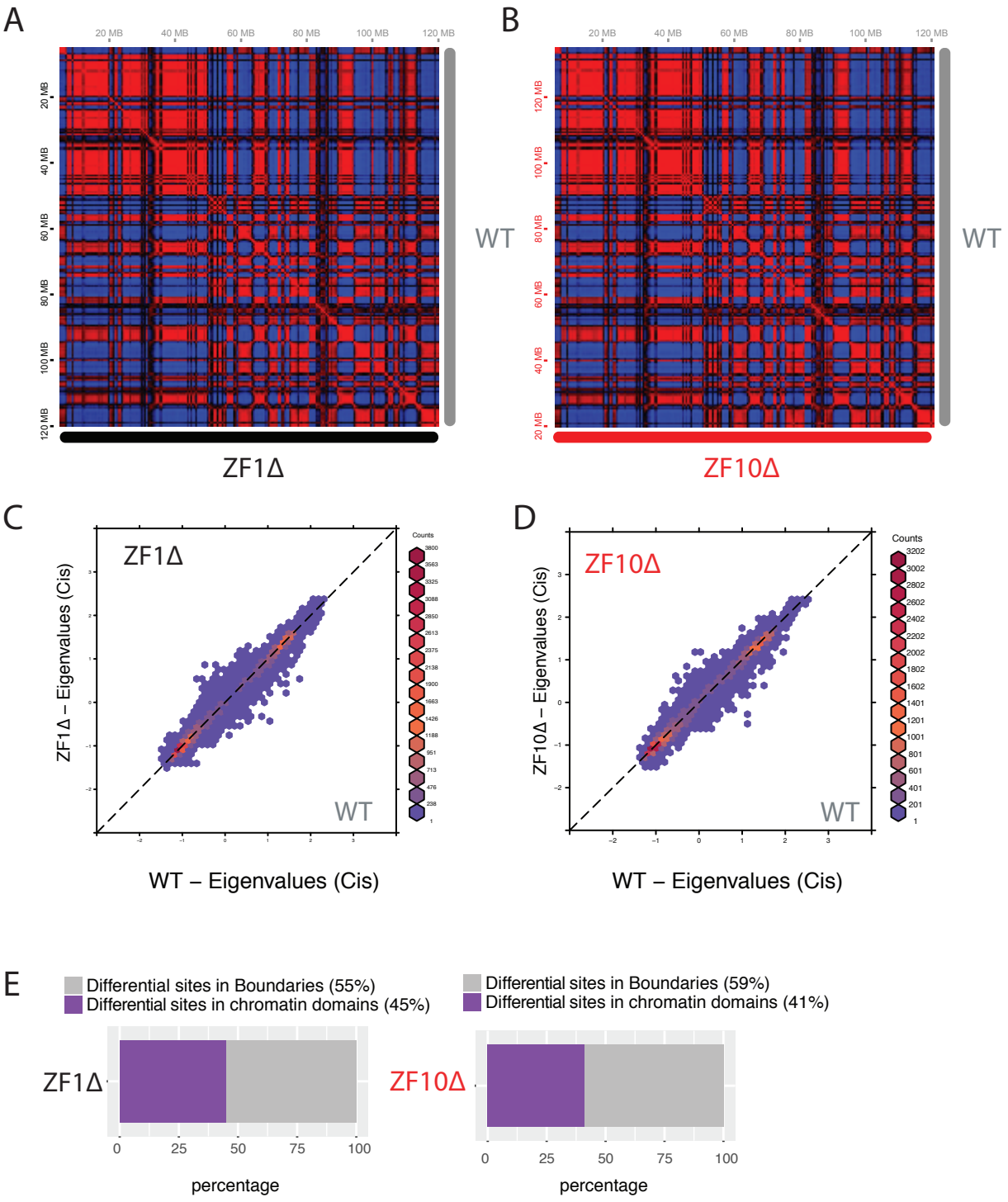

Figure S6 related to Figure 6. Genomic compartmentalization is unaffected by RBR mutants
(A and B) Representative Pearson's correlation maps [(A), ZF1 vs WT and (B), ZF10Δ vs WT] of chromosome 12 showing the plaid pattern fine-scale compartmentalization is unaffected. (C and D) Comparison of distributions of cis-Eigenvector 1 values showing no difference between conditions [(C), ZF1Δ vs WT and (D), ZF10Δ vs WT). (F) Bar graph representing the distribution of differential binding sites for ZF1Δ and ZF10Δ.